

Particle velocity gradient based acoustic mode beamforming for short linear vector sensor arrays^{a)}

Berke Gur^{b)}

Department of Mechatronics Engineering, Bahcesehir University, Istanbul, Turkey

(Received 28 October 2013; revised 4 April 2014; accepted 30 April 2014)

In this paper, a subtractive beamforming algorithm for short linear arrays of two-dimensional particle velocity sensors is described. The proposed method extracts the highly directional acoustic modes from the spatial gradients of the particle velocity field measured at closely spaced sensors along the array. The number of sensors in the array limits the highest order of modes that can be extracted. Theoretical analysis and numerical simulations indicate that the acoustic mode beamformer achieves directivity comparable to the maximum directivity that can be obtained with differential microphone arrays of equivalent aperture. When compared to conventional delay-and-sum beamformers for pressure sensor arrays, the proposed method achieves comparable directivity with 70%–85% shorter apertures. Moreover, the proposed method has additional capabilities such as high front–back (port–starboard) discrimination, frequency and steer direction independent response, and robustness to correlated ambient noise. Small inter-sensor spacing that results in very compact apertures makes the proposed beamformer suitable for space constrained applications such as hearing aids and short towed arrays for autonomous underwater platforms.

© 2014 Acoustical Society of America. [<http://dx.doi.org/10.1121/1.4876180>]

PACS number(s): 43.60.Fg, 43.58.Fm [ZHM]

Pages: 3463–3473

I. INTRODUCTION

The acoustic field is described with two separate variables: the scalar pressure and the vectorial particle velocity variables. The pressure variable is significantly simpler to measure. Therefore, a majority of the existing acoustic applications rely on omni-directional pressure sensors. However, being a scalar variable, pressure measurements at a point in space do not provide directional information regarding the acoustic field. Therefore, linear arrays of omni-directional pressure sensors are used for signal enhancement, interference suppression, and direction-of-arrival (DOA) estimation (Van Veen and Buckley, 1988; Krim and Viberg, 1996). The directivity of the array improves as the aperture length is increased. To avoid grating lobes and provide robustness against ambient noise, the separation between the pressure sensors in the array is generally set at one-half of the acoustic wavelength. In its simplest form, data independent delay-and-sum beamforming is implemented by time delaying each sensor measurement according to the desired steer direction. As a result, incoming waves are summed constructively to form the array output. Other more advanced data dependent, adaptive, and optimum beamformers also rely on the additive processing of sensor measurements (Van Veen and Buckley, 1988). In contrast, subtractive beamformers differentially process time delayed pressure measurements obtained from arrays with inter-sensor spacing much less than the wavelength. Subtractive beamformers offer several advantages

over the conventional additive beamformers such as super-directivity (i.e., higher directivity for a given aperture length), better noise, and cross-talk rejection (Elko, 2004).

The particle velocity has historically been neglected, despite providing directional information regarding the acoustic field. This can be attributed to the lack of affordable sensors capable of reliable measurements. However, the demand for higher performance array systems, coupled with the recent advancements in single crystal ceramic and microelectromechanical systems sensor fabrication technology, has resulted in the development of particle velocity sensors (Shipps and Deng, 2003; Jacobsen and de Bree, 2009). In general, particle velocity sensors are combined with pressure sensors in a single package to form an acoustic vector sensor (AVS). Although there is substantial literature on additive beamformers for velocity sensor arrays, subtractive beamformers for such arrays are neglected. In this paper, a subtractive beamformer suitable for short and linear two-dimensional (2-D) velocity sensor arrays is presented.

Subtractive beamformers designed for audio (Teutsch, 2007), telecommunication (Elko, 1996), and biomedical (Kates, 1993; Thompson, 2003; Chung *et al.*, 2006) applications are generally referred to as differential microphone arrays. The inter-sensor separations and time delays in differential arrays are small relative to the wavenumber and the sampling rate, respectively. An N th order differential array can be obtained from closely spaced $M = N + 1$ omni-directional pressure sensors. The maximum directivity that can be achieved with differential arrays with M sensors is $2M - 1$ for 2-D and M^2 for three-dimensional (3-D) isotropic noise (Elko, 2004). These results are in agreement with the theoretical upper directivity limit of M^2 for an array of M omni-directional sensors. It should also be noted that this value for the maximum directivity is achieved for linear

^{a)}Portions of this work were presented in “Gradient based processing of linear vector sensor arrays,” Proceedings of 11th European Conference on Underwater Acoustics (ECUA 2012), Edinburgh, Scotland, July 2012.

^{b)}Author to whom correspondence should be addressed. Electronic mail: berke.gur@eng.bahcesehir.edu.tr

arrays steered to the endfire direction (Weston, 1986; Parsons, 1987). Several optimum differential array design methods based on maximizing various performance metrics exist. Commonly used performance metrics are directivity, front-back (port-starboard) ratio, and main beam width. A concise review of the optimal differential microphone array designs based on these performance metrics are provided by Elko (2004). More recently, De Sena *et al.* (2012) developed a differential array design methodology based on the weighted optimization of the frontal and back sector directivity ratios and the smoothness of the directivity function in the frontal sector. Most practical realizations of differential arrays found in the literature are limited to an order of three or less (e.g., see Elko, 2004 and De Sena *et al.*, 2012). This is due to adverse effects of electronic noise and microphone mismatch at higher orders. Abhayapala and Gupta (2010) proposed an alternative differential array design scheme which alleviates the effects of electronic noise and enables practical array realizations above third order. Although the nulls can be steered (Elko, 2004), the main response axis differential microphone arrays is confined to the array axis and cannot be steered (Teutsch, 2007). This inability to steer the main response axis is one of the major limitations of differential arrays.

An alternative perspective on differential arrays considers them as higher order acoustic sensors capable of measuring the spatial gradients of the pressure field. Spatial gradients naturally arise from the Taylor series expansion of the pressure field at a point (Cray *et al.*, 2003; Schmidlin, 2007). These conceptual higher order acoustic sensors have the same response function and directivity as differential arrays. The equivalence of differential arrays and gradient based higher order acoustic sensors is briefly mentioned by Olson (1946) and firmly established by Kolundzija *et al.* (2011). Cox and Lai developed design methods based on simultaneous optimization of array and white noise gains for linear arrays of higher order sensors (Cox and Lai, 2007). The authors extended their design methodology to simultaneous grating and back lobe rejection (Cox and Lai, 2009). Kasilingam *et al.* (2009) proposed a linear prediction based estimation of the higher order spatial gradients from lower order gradient measurements of the acoustic field. A closed form DOA estimation method for a general 3-D n th order acoustic sensor is described by Song and Wong (2012). Lai and Bell (2007) derived Cramer-Rao bounds on the DOA estimates obtained from arrays of higher order acoustic sensors.

As a practical realization of higher order acoustic sensors, a subtractive planar beamformer for underwater linear arrays based on the gradients of the pressure field is proposed by Franklin (1997). The author derives optimal weights that maximize the directivity of the subtractive array for various underwater noise fields. The resulting super-directive linear array achieves directionality comparable to conventional additive pressure sensing arrays with much shorter aperture. More specifically, the necessary aperture length of an equivalent conventional array is computed to be between 14 (at 200 Hz) to 1.4 times (at 9 kHz) longer than the super-directive array. However, as with differential microphone arrays, the main response axis of the proposed super-directive array is in the endfire direction and cannot be steered, limiting the applicability of the method.

Motivated by the advent of high performance AVS in the last decade, in particular, for underwater acoustic applications, there has been a surge in the research on linear AVS arrays. Cray and Nuttall (2001) describe several beamforming approaches for linear AVS arrays, where the inter-sensor spacing is set to half the wavelength. In particular, the authors propose a method where each AVS in the array is individually beamformed to produce a standard steerable cardioid response. These individual AVS responses are then combined using the delay-and-sum method to obtain the array response. A major conclusion is that linear AVS arrays, albeit equipped with more measurement channels, provide a directivity improvement of up to 5 dB compared to conventional arrays of equal aperture lengths. More recently, Smith and Van Leijen (2007) proposed a beamformer by extending on the cardioid pattern of a single AVS in the array. In the method proposed by the authors, the cardioid response of a single AVS is raised to integer powers, resulting in a more directional single sensor response. Again, the individual sensor responses from the half-wavelength spaced AVS are combined using the delay-and-sum method. In a series of papers by Nehorai on DOA estimation using AVS arrays, inter-sensor separations of half-wavelength or more are assumed (Nehorai and Paldi, 1994; Hawkes and Nehorai, 1998). Chen and Zhao (2004) present an extension of the minimum variance distortionless response beamformer to AVS arrays with inter-sensor separation of one-half of the wavelength or more. An acoustic mode processor for a single AVS is described in Clark (2008). However, *a priori* knowledge of the DOA of the acoustic wave is required for the processor, limiting the practical applicability of the method. Existing scientific literature on AVS arrays is overwhelmingly based on the traditional design of half-wavelength spacing employed for pressure arrays. However, this design is not necessarily justified in terms of noise suppression for AVS arrays (D'Spain *et al.*, 2006).

This paper presents a subtractive beamformer for short linear velocity sensor arrays. The proposed method overcomes the limitation of the main response axis being restricted to the endfire direction present in existing subtractive and differential arrays. Furthermore, the beamformer relies on arrays with inter-sensor separation much smaller than one-half of the wavelength, enabling more compact arrays. The paper is organized as follows. A theoretical treatment of the proposed method, including the approximation of the velocity gradients using finite differences, the extraction of the acoustic modes, and their processing to obtain directional beam responses are presented in Sec. II. The performance and directivity analysis of the proposed beamformer are provided in Sec. III. The effects of sensor spacing and ambient noise on array performance, as well as alternative array configurations are discussed. The paper is concluded in Sec. IV with a summary and discussion of future work.

II. THEORETICAL DEVELOPMENT

A. The acoustic field

Consider a short uniform linear array of particle velocity sensors placed along the x -axis of a Cartesian coordinate

system (as shown in Fig. 1). Each sensor in the array is capable of making particle velocity measurements in the x - y plane of the array. The array also incorporates a single pressure sensor located at the array center. A planar time-harmonic wave with an angular frequency of $\omega = kc$ (k is the wavenumber and c is the speed of sound) is incident to the array at an azimuth angle of ψ . The azimuth angle is measured from the x -axis with the positive sense in the counterclockwise direction toward the y -axis. For this 2-D setup, the elevation angle, θ (measured in the positive sense from the y -axis toward the z -axis), is zero for the incoming wave. The vertical separation between the source and array is small compared to the horizontal separation in room teleconferencing and shallow water marine applications. These are typical cases that involve plane waves traveling in a 2-D acoustic field. The pressure and particle velocity at any point, x , along the array axis [omitting the time dependent part $\exp(j\omega t)$] can be expressed as (Cray and Nuttall, 2001; Ziomek, 1995)

$$\begin{aligned} p(x) &= P \exp(jk \cos \psi x), \\ v_x(x) &= V \cos \psi \exp(jk \cos \psi x), \\ v_y(x) &= V \sin \psi \exp(jk \cos \psi x), \end{aligned} \quad (1)$$

where P and V are the amplitudes of the pressure and velocity field variables, and ψ is the azimuth angle as defined previously. The spatial gradients of the particle velocities in Eq. (1) are

$$\begin{aligned} \frac{\partial^n v_x}{\partial x^n} &= V(jk)^n \cos \psi (\cos \psi)^n \exp(jk \cos \psi x), \\ \frac{\partial^n v_y}{\partial x^n} &= V(jk)^n \sin \psi (\cos \psi)^n \exp(jk \cos \psi x). \end{aligned} \quad (2)$$

Evaluating the n th order gradients given in Eq. (2) at the center of the array (i.e., at $x = 0$) results in

$$\begin{aligned} \frac{\partial^n}{\partial x^n} v_x(0) &= V(jk)^n (\cos \psi)^{n+1}, \\ \frac{\partial^n}{\partial x^n} v_y(0) &= V(jk)^n \sin \psi (\cos \psi)^n. \end{aligned} \quad (3)$$

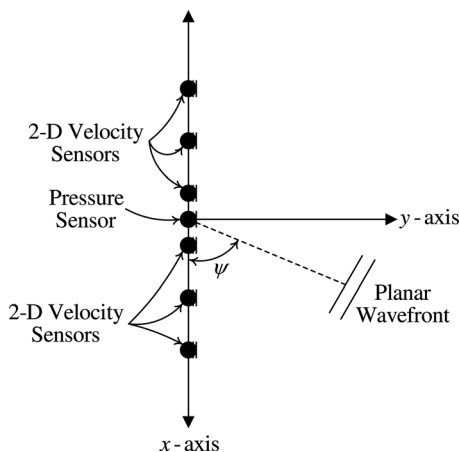


FIG. 1. The Cartesian coordinate system and the AVS array.

The x -direction spatial gradients of the particle velocity field evaluated at the origin are required in the derivation of the proposed beamformer (as explained in Sec. II C). However, there are no acoustic sensors that can directly measure the spatial gradients of the particle velocity. Instead, the spatial gradients at the origin are approximated from measurements made by the array of particle velocity sensors using finite differences. The utility of the single pressure sensor at the array center is explained in Sec. II D.

B. Approximating the particle velocity gradients with finite differences

The first derivative of any spatial function, $v(\xi)$, can be approximated in terms of the first order central difference {i.e., $\partial v(\xi)/\partial x \approx [v(\xi + d/2) - v(\xi - d/2)]/d$, for very small d }. Likewise, it is possible to approximate the second derivative by taking the central finite difference of two first order central finite differences {i.e., $\partial^2 v(\xi)/\partial x^2 \approx [v(\xi + d) - 2v(\xi) + v(\xi - d)]/d^2$ }. Extending on this approach, any higher order gradient, $\partial^n v(\xi)/\partial \xi^n$, can be obtained from the finite difference operator

$$g_n[v(\xi)] = \frac{\delta_n[v(\xi)]}{d^n}, \quad (4)$$

where the $\delta_n(\cdot)$ operator is defined as

$$\delta_n[v(\xi)] = \sum_{l=0}^n (-1)^{n-1} \binom{n}{l} v[\xi + (l - n/2)d]. \quad (5)$$

The coefficients of the $\delta_n(\cdot)$ operator are the binomial coefficients

$$\binom{n}{l} = \frac{n!}{l!(n-l)!}. \quad (6)$$

In the context of this paper, $v(\xi)$ is the particle velocity evaluated at some point $x = \xi$ along the x -axis, n is the order of the gradient, and d is the separation between the sensors. Thus, for small sensor spacing relative to the wavelength (i.e., $kd/2 = \pi d/\lambda \ll 1$), the n th order gradient of the particle velocity evaluated at the origin can be approximated with the n th order finite difference operation $g_n(\cdot)$ {e.g., $\partial^n v_x(0)/\partial x^n \approx g_n[v_x(0)]$ }. Table I outlines the parameters of the finite difference operator, $g_n(\cdot)$, used for approximating the first five gradients of the acoustic field variables.

C. Extracting acoustic modes from the field variable gradients

The velocity gradients defined in Eq. (2) can be approximated from measurements made at sensors using the finite difference operator, $g_n(\cdot)$. These gradients for the x - and y -direction particle velocities involve the trigonometric terms $(\cos \psi)^{n+1}$ and $\sin \psi (\cos \psi)^n$, respectively. The n th spatial gradient of the x -direction particle velocity evaluated at the origin, $x = 0$ [given in Eq. (3)], can be expanded as (see the Appendix for the derivation)

TABLE I. The parameters of the finite difference operator, $g_n(\cdot)$, used for approximating the first few gradients of the acoustic field variables.

Gradient order (n)	Required measurement locations ($\xi = 0$) ($l = n/2$)	Corresponding binomial coefficients $(-1)^{(n-l)} [n! / (l!(n-l)!)]$
0	0	1
1	$+d/2, -d/2$	$+1, -1$
2	$+d, 0, -d$	$+1, -2, +1$
3	$+3d/2, +d/2, -d/2, -3d/2$	$+1, -3, +3, -1$
4	$+2d, +d, 0, -d, -2d$	$+1, -4, +6, -4, +1$
5	$+5d/2, +3d/2, +d/2, -d/2, -3d/2, -5d/2$	$-1, +5, -10, +10, -5, +1$

$$\frac{\partial^n}{\partial x^n} v_x(0) = V(jk)^n \cdot \begin{cases} \left[\frac{2}{2^{n+1}} \sum_{l=0}^{n/2} \binom{n+1}{l} \cos[(n-2l+1)\psi] \right], & n \text{ even} \\ \left[\frac{2}{2^{n+1}} \sum_{l=0}^{(n-1)/2} \binom{n+1}{l} \cos[(n-2l+1)\psi] + \frac{1}{2^{n+1}} \binom{n+1}{(n+1)/2} \right], & n \text{ odd,} \end{cases} \quad (7)$$

where the $\cos[(n-2l+1)\psi]$ terms are the cosine modes of the acoustic field. Note that if n is even, the summation will include only the odd ordered cosine modes less than or equal to $n+1$ [e.g., if $n=4$, cosine modes included in the summation will be $\cos(\psi)$, $\cos(3\psi)$, and $\cos(5\psi)$]. If n is odd, the summation will include only the even ordered cosine modes

less than or equal to $n+1$ and a constant term [e.g., if $n=5$, cosine modes included in the summation will be $\cos(2\psi)$, $\cos(4\psi)$, $\cos(6\psi)$, and a constant term].

Likewise, the n th spatial gradient of the y -direction particle velocity evaluated at the origin, $x=0$, can be expanded as (see the Appendix for the derivation)

$$\frac{\partial^n}{\partial x^n} v_y(0) = V(jk)^n \cdot \begin{cases} \left[\frac{1}{2^n} \sum_{l=0}^{n/2} \left[\frac{n!(n-2l+1)}{l!(n-l+1)!} \right] \sin[(n-2l+1)\psi] \right], & n \text{ even} \\ \left[\frac{1}{2^n} \sum_{l=0}^{(n-1)/2} \left[\frac{n!(n-2l+1)}{l!(n-l+1)!} \right] \sin[(n-2l+1)\psi] \right], & n \text{ odd,} \end{cases} \quad (8)$$

where the $\sin[(n-2l+1)\psi]$ terms are the sine modes of the acoustic field. If n is even, the summation in Eq. (8) will include only the odd ordered sine modes less than or equal to $n+1$ [e.g., if $n=4$, sine modes included in the summation will be $\sin(\psi)$, $\sin(3\psi)$, and $\sin(5\psi)$].

If n is odd, the summation will include only the even ordered sine modes less than or equal to $n+1$ [e.g., if $n=5$, sine modes included in the summation will be $\sin(2\psi)$, $\sin(4\psi)$, and $\sin(6\psi)$].

D. The velocity gradient acoustic mode beamforming algorithm

As can be seen from Table I, the sensor locations necessary to approximate the even and odd ordered gradients do not coincide. This suggests that to be able to approximate up to the N th order gradient, one needs $M=2N+1$ sensors separated by a distance of $d/2$. However, by shifting the reference center for the even numbered modes by a distance of

$d/2$ in the positive x -direction, it is possible to use the same sensors for estimating both the even and odd numbered gradients (Franklin, 1997). Assuming that the incident wave is a plane wave, the shift in the reference center can be corrected by time delaying the even order gradients by $d \cos \psi_s / 2c$, where ψ_s is the desired azimuth steer angle. As a consequence, it is possible to estimate up to the N th order gradient using $M=N+1$ sensors separated by a distance of d (see Fig. 2).

Once the gradients at $x=0$ are computed from finite differences (as outlined in Sec. II B), each gradient is weighted by a normalization factor, $a_n = (jk)^{-n}$. This normalization is performed to compensate for the $(jk)^n$ terms appearing in Eq. (3). Following normalization, the gradients are filtered to steer the beamformer in the desired direction. The x - and y -direction velocity gradients are processed using separate filters with coefficients $w_{x,n}$ and $w_{y,n}$, respectively. Following the filtering, the gradients are summed resulting in the beamformer output of the form

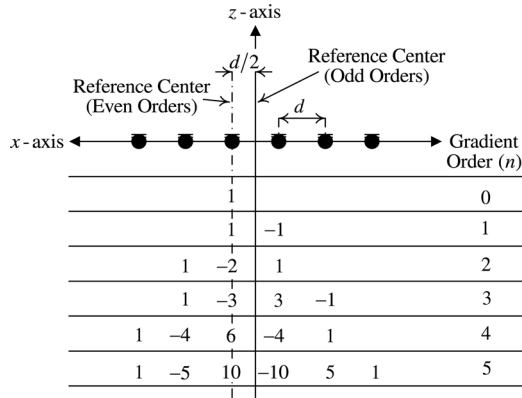


FIG. 2. Practical realization of a six sensor vector sensor array (pressure sensor omitted for clarity) depicting the sensor weights for approximating the first six gradients.

$$\sum_{n=0}^N w_{x,n} V (\cos \psi)^{n+1} + \sum_{n=0}^N w_{y,n} V \sin \psi (\cos \psi)^n. \quad (9)$$

The choice of the filter weights affects the beamformer response and array directivity. The filter weights can be chosen to maximize a performance metric such as directivity, front-back (port-starboard) ratio, main beam width, grating and back lobe suppression, and white noise gain (Franklin, 1997; Elko, 2004; Cox and Lai, 2007; Cox and Lai, 2009). An alternative is to choose the filter weights such that the beamformer output corresponds to a certain desired response function. The latter approach is pursued in this paper with a desired beamformer response in the form of

$$r(\psi_s) \propto \sum_n \cos[n(\psi - \psi_s)], \quad (10)$$

which attains a maximum value at $\psi_s = \psi$ and has some properties such as good side-lobe suppression and high front-back ratio. Since the contribution of each x -direction gradient order to the cosine modes are readily available from Eq. (7), it is possible to construct the $(N+1) \times (N+1)$ matrix

$$\mathbf{A}_x = \begin{bmatrix} a_x(1,0) & a_x(1,1) & \cdots & a_x(1,N) \\ a_x(2,0) & a_x(2,1) & \cdots & a_x(2,N) \\ \vdots & \vdots & \ddots & \vdots \\ a_x(N+1,0) & a_x(N+1,1) & \cdots & a_x(N+1,N) \end{bmatrix}, \quad (11)$$

whose elements $a_x(l,n)$ represent the contribution of the n th order x -direction gradient (i.e., $\partial^n v_x / \partial x^n$) to the $\cos(l\psi)$ term. Likewise, using Eq. (8), it is possible to construct a similar $(N+1) \times (N+1)$ matrix \mathbf{A}_y with elements $a_y(l,n)$ representing the contribution of the n th order y -direction gradient (i.e., $\partial^n v_y / \partial x^n$) to the $\sin(l\psi)$ term. Defining the two $(N+1) \times 1$ steering vectors, \mathbf{b}_x and \mathbf{b}_y , such that

$$\mathbf{b}_x = \begin{bmatrix} \cos \psi_s \\ \cos(2\psi_s) \\ \vdots \\ \cos[(N+1)\psi_s] \end{bmatrix}, \quad \mathbf{b}_y = \begin{bmatrix} \sin \psi_s \\ \sin(2\psi_s) \\ \vdots \\ \sin[(N+1)\psi_s] \end{bmatrix}, \quad (12)$$

it is possible to obtain an exact solution for the x - and y -direction filter weights, $w_{x,n}$ and $w_{y,n}$, $n = 1, 2, \dots, N$, corresponding to the non-zero gradient orders by solving the determined set of equations

$$\begin{bmatrix} \mathbf{A}_x & \mathbf{0}_{N \times N} \\ \mathbf{0}_{N \times N} & \mathbf{A}_y \end{bmatrix} \begin{bmatrix} \mathbf{w}_x \\ \mathbf{w}_y \end{bmatrix} = \begin{bmatrix} \mathbf{b}_x \\ \mathbf{b}_y \end{bmatrix}, \quad (13)$$

where $\mathbf{w}_x = [w_{x,0} \ w_{x,2} \ \cdots \ w_{x,N}]^T$ and $\mathbf{w}_y = [w_{y,0} \ w_{y,2} \ \cdots \ w_{y,N}]^T$ are the $(N+1) \times 1$ filter weight vectors and $\mathbf{0}_{N \times N}$ is the square zero matrix of size N . The resulting beamformer output takes the form

$$V \cdot \sum_{n=1}^{N+1} [\cos(n\psi) \cos(n\psi_s) + \sin(n\psi) \sin(n\psi_s)] + V \cdot \sum_{n=1}^{(N+1)/2} \frac{1}{2^{2n-1}} \binom{2n-1}{n} w_{x,2n-1}. \quad (14)$$

The second term in Eq. (14) is due to constant terms arising in the odd gradients of the x -direction particle velocity [see Eq. (7)]. This constant term must be made equal to unity for the array response to reduce to the desired form given in Eq. (10). If left as is, the constant term results in a distortion in the beampattern. A correction for the distortion can be derived by first noting that the constant term in Eq. (14) can be expressed as $V \mathbf{a}_x \mathbf{w}_x$. The elements $a_x(0,n)$ of the $1 \times (N+1)$ vector, \mathbf{a}_x , are defined similar to the elements of the \mathbf{A}_x matrix. The vectors \mathbf{a}_x and \mathbf{w}_x can be computed from Eqs. (7) and (13), respectively. However, the particle velocity amplitude (V) is not readily available from the velocity measurements. To overcome this problem, a single pressure measurement made at the array center can be utilized. For plane waves, the pressure and particle velocity amplitudes are related through $p(0)/\rho c = P/\rho c = V$ (where ρ is the density of the medium). Thus, the correction can be accomplished by subtracting the term

$$Q = \frac{p(0)}{\rho c} (\mathbf{a}_x \mathbf{w}_x - 1), \quad (15)$$

from the array response. For this purpose, a dedicated pressure sensor can be incorporated into the array at the origin (as shown in Fig. 1). Alternatively, one of the central 2-D velocity sensors can be replaced with a 2-D AVS capable of making collocated measurements of the pressure and particle velocity fields. Time-shifted (to the array center) pressure measurements from this AVS can then be used for the correction. After the correction, the beamformer output takes the form

$$y = V \sum_{n=0}^{N+1} \cos[n(\psi - \psi_s)], \quad (16)$$

which is in the form of the response given in Eq. (10). Without the loss of generality, the particle velocity amplitude is taken as unity (i.e., $V = 1$). It is desirable to normalize the array response such that it has a value of unity in the

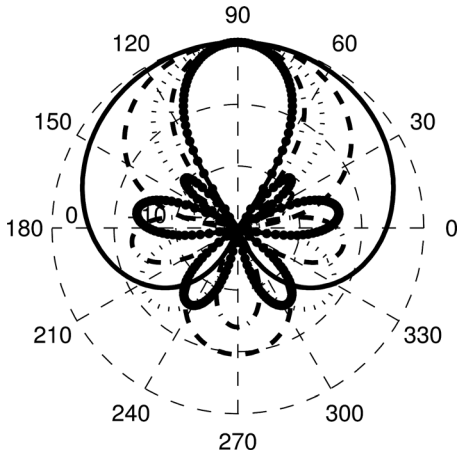


FIG. 3. A logarithmic polar plot showing the beampatterns obtained using the proposed method for a single vector sensor (solid), and arrays consisting of two (dashed), three (dotted), four (dashed-dotted), and five (connected plus) AVS.

steer direction. Noticing that $M = N + 1$, the resulting normalized beamformer response becomes

$$r(\psi_s) = \frac{1}{M+1} \sum_{n=0}^M \cos[n(\psi - \psi_s)]. \quad (17)$$

Theoretical beampatterns for the array can be obtained as the magnitude squared of the array response, $B(\psi, \theta) = |r(\psi, \theta)|^2$. Such beampatterns for arrays comprised of five or less vector sensors (steered to broadside) are shown in Fig. 3. As can be predicted from Eq. (17), the response

reduces to the standard cardioid response for a single sensor (i.e., 2-D AVS). Arrays with odd number of sensors provide perfect port-starboard discrimination (front-back ratio). Even number of sensors results in lower discrimination (-10 dB for $M = 2$ and decreasing with increasing number of sensors). Theoretical beampatterns for a six sensor array steered in the azimuthal direction are shown in Fig. 4. Simulated beampatterns for a six AVS short underwater array (sensor spacing 0.1 m, acoustic aperture length 0.5 m), obtained by processing 0.5 kHz time-harmonic signals corrupted with 3-D isotropic ocean noise (with signal-to-noise ratio of 10 dB), are also presented on the same figure.

III. PERFORMANCE ANALYSIS

A. Finite difference errors

The finite difference error made in approximating the spatial gradients with finite differences (defined as the ratio of the finite difference approximation and the true theoretical gradient) for order n is given as

$$e_n(\psi) = \left[\frac{\sin[(kd/2) \cos \psi]}{(kd/2) \cos \psi} \right]^n. \quad (18)$$

This error is plotted for a plane wave incident with $\psi = 0$ as of a function of the sensor spacing for different gradient orders in Fig. 5. For a given sensor spacing, d , increasing frequency (i.e., reducing the wavelength, λ , or increasing k) results in an increase in the finite difference error. Hence, the proposed beamformer is more suited for processing low

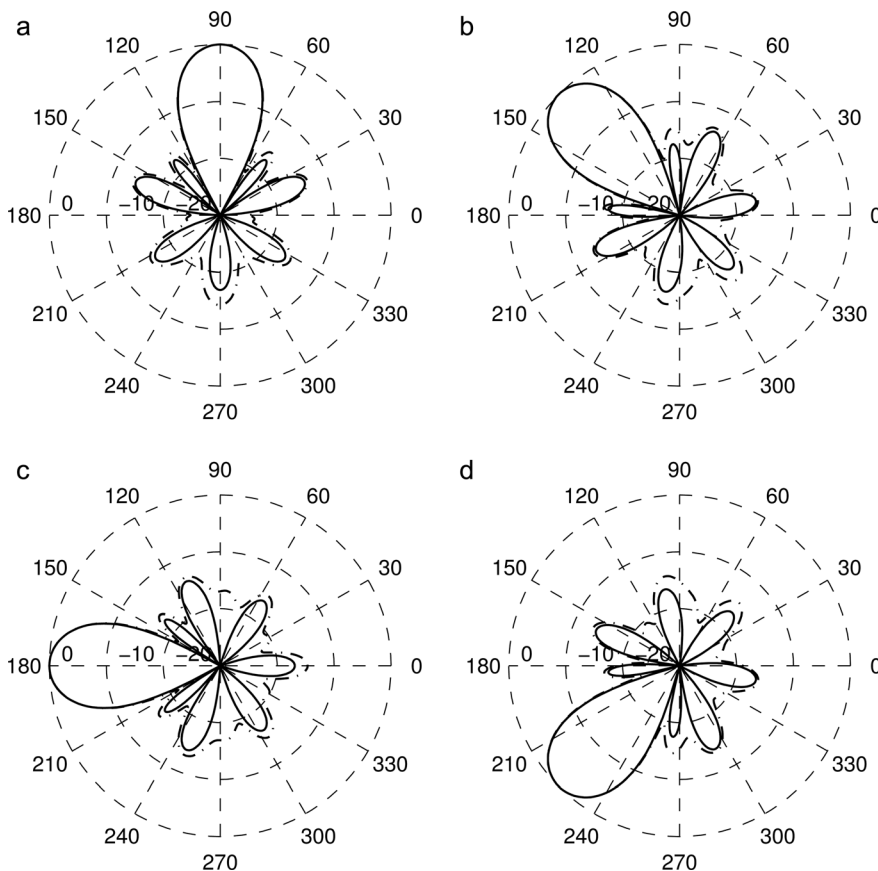


FIG. 4. The theoretical (solid) and simulated (with signal-to-noise ratio of 10 dB; dashed-dotted) beampatterns of a short array of six 2-D vector sensors steered toward (a) 90 (broadside), (b) 135 , (c) 180 (endfire), and (d) 210 degrees.

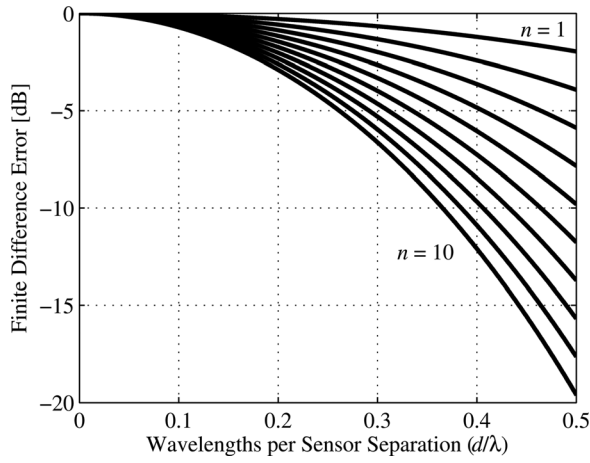


FIG. 5. The finite difference approximation error for each gradient order (n) as a function of the relative sensor spacing (d/λ).

frequency signals. For a given sensor spacing and frequency, the finite difference approximation error also increases with increasing order, n . This is due to accumulation of finite differencing errors with increasing gradient orders. In designing high order arrays and establishing the upper operating frequency limits, the accumulative nature of the finite difference errors must be taken into account.

B. Directivity calculations

The directivity function for a receiver array can be defined in terms of the array response as

$$D(\psi) = \frac{r(\psi)}{r(\psi_{\max})}, \quad (19)$$

where ψ_{\max} is the azimuth direction of the maximum response. Assuming that the wave is incident at an azimuth of $\psi = 0$ and redefining the steer azimuth angle as $\psi_s \triangleq \psi$, the array response given in Eq. (17) becomes

$$r(\psi) = \frac{1}{M+1} \sum_{n=0}^M \cos(n\psi). \quad (20)$$

Substituting Eq. (20) into Eq. (19), the directivity function is computed as

$$D(\psi) = \frac{1}{M+1} \sum_{n=0}^M \cos(n\psi). \quad (21)$$

Using Lagrange's trigonometric identity, Eq. (21) simplifies to

$$D(\psi) = \frac{1}{2(M+1)} + \frac{\sin[(M+1/2)\psi]}{2(M+1)\sin(\psi/2)}. \quad (22)$$

The directivity function given in Eq. (22) results in a half-power beamwidth of $\psi_{-3\text{dB}} = 155^\circ/M$. This result is in agreement with the beamwidth reported by Clark (2008).

Array gain (AG) is defined as the improvement in signal-to-noise ratio resulting from the beamformer relative to a

single omni-directional pressure sensor and is computed using the relation

$$\text{AG} = \frac{\int_0^{2\pi} d\psi \int_{-\pi/2}^{\pi/2} F(\psi, \theta) \cos \theta d\theta}{\int_0^{2\pi} d\psi \int_{-\pi/2}^{\pi/2} B(\psi, \theta) F(\psi, \theta) \cos \theta d\theta}, \quad (23)$$

where $F(\psi, \theta)$ is the intensity directivity of the noise field. Assuming a 2-D isotropic noise field characterized by $F(\psi, \theta) = \delta(\theta)$, the AG becomes

$$\text{AG}_{2\text{D}} = \frac{2\pi(M+1)^2}{\int_0^{2\pi} \left[\sum_{n=0}^M \cos(n\psi) \right]^2 d\psi} = \frac{2(M+1)^2}{M+2}. \quad (24)$$

The directivity factor (DF) is defined as the AG in 3-D isotropic noise characterized by the directivity of $F(\psi, \theta) = 1$. The directivity index is calculated as $10 \log_{10}(\text{DF})$ and evaluated numerically for the proposed beamformer. The results are presented graphically in Fig. 6 as a function of the number of sensors, M . In Fig. 6, it is assumed that the array configuration satisfies $kd \ll 1$. For high frequencies, the non-dimensional variable, kd , approaches and eventually exceeds unity. In that case, the error associated with approximating the particle velocity gradients with finite differences becomes significant. As a consequence, the performance of the beamformer decreases. The AG is numerically evaluated and plotted in Fig. 7 as a function of frequency for underwater arrays with different number of sensors (and with a 0.1 m sensor spacing). From Fig. 7, it is observed that the directivity of the array does not vary significantly with frequency at low frequencies where $kd \leq 1$. Thus, the proposed beamformer is frequency independent, provided that the sensor spacing criteria for accurate gradient estimation is satisfied. Frequency independent response is also evident from the theoretical array response function derived in Eq. (17).

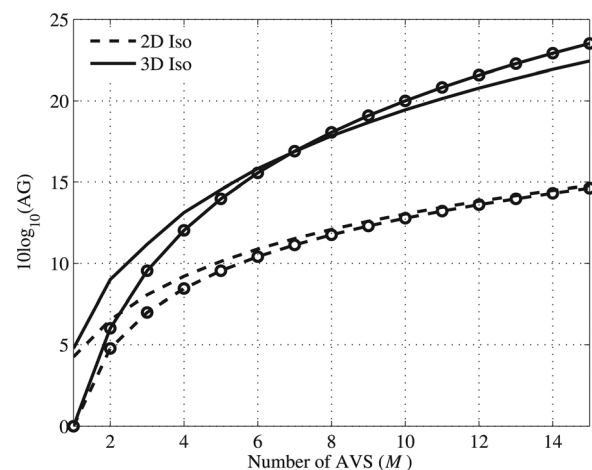


FIG. 6. AG as a function of the number of sensors for 2-D and 3-D isotropic noise. The lines without markers are for the proposed method, lines marked with open circles represents the theoretical upper directivity limit of differential microphone arrays.

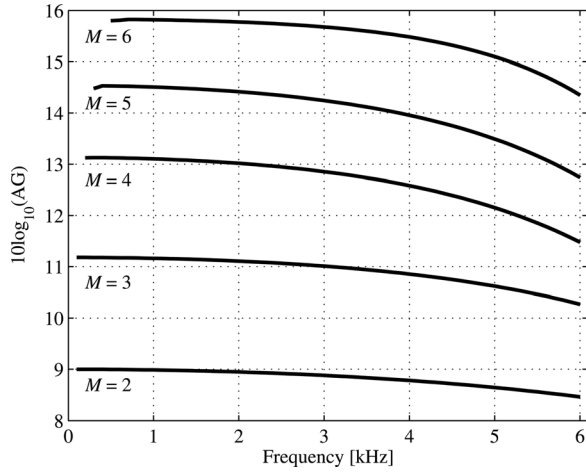


FIG. 7. AG as a function of frequency for arrays of different number of sensors (M) for 3-D isotropic underwater noise.

C. Effects of spatially correlated noise

Conventional pressure based additive beamformers achieve optimum AG if noise measured at the sensors are uncorrelated. The spatial cross-spectrum of pressure in a 3-D isotropic noise field is given by $S_{pp}(d, \omega) = j_0(kd) \cdot S_p(\omega)$ where $j_0(x) = \sin x/x$ is the spherical Bessel function of zeroth order and $S_p(\omega)$ is the noise pressure autospectrum. The oscillatory function, $j_0(kd)$, has a decreasing envelope and is equal to zero at integer multiples of half the wavelength. Thus, to optimize the AG, inter-element spacing in uniform linear arrays of pressure sensors is generally set to half the design wavelength (D'Spain *et al.*, 2006). The proposed subtractive beamformer attains optimum directivity in the presence of correlated ambient noise. For the orientation shown in Fig. 1, D'Spain *et al.* (2006) shows that the particle velocity spatial cross-spectra in a 3-D isotropic noise field are

$$\begin{bmatrix} S_{xx}(d, \omega) \\ S_{yy}(d, \omega) \\ S_{zz}(d, \omega) \end{bmatrix} = \begin{bmatrix} j_1(kd)/kd - j_2(kd) \\ j_1(kd)/kd \\ j_1(kd)/kd \end{bmatrix} \frac{S_p(\omega)}{(\rho c)^2}, \quad (25)$$

where $j_1(x) = \sin x/x^2 - \cos x/x$ and $j_2(x) = (3/x^2 - 1) \times (\sin x/x) - 3 \cos x/x^2$ are spherical Bessel functions of the first and second orders, respectively. Spatial cross-spectra between orthogonal particle velocity components, and between pressure and particle velocity components are zero except for $S_{px}(d, \omega)$, which is proportional to $j_1(kd)$. The functions, $j_1(kd)$ and $j_2(kd)$, are also oscillatory with decreasing envelopes. This decreasing envelope causes the performance of the proposed beamformer to decrease with increasing inter-element spacing and increasing frequency. Hence, small inter-element spacing is not only required for accurate particle velocity spatial gradient estimation (as explained in Sec. II B), but is also important for achieving high AG and good ambient noise rejection. In addition, sampling rates higher than necessary will introduce high frequency noise with low spatial correlation into the beamformer, again reducing directivity and performance. Uncorrelated signals result from channel mismatch, errors in microphone spacing, local flows, and electronic circuitry.

Such signals are known to adversely affect the performance of the proposed method (e.g., see Franklin, 1997). A detailed analysis of the effects of such uncorrelated noise on beamformer performance is not included in this paper and will be addressed in future work.

D. Comparison with existing methods

As the proposed beamformer represents a viable alternative to gradient and differential microphone arrays, it is worth comparing their directivities. It is noted in Sec. I that the maximum achievable directivity of differential microphone arrays with M sensors is $2M-1$ for 2-D, and M^2 for 3-D isotropic noise. For comparison, these directivity values of differential arrays are plotted in Fig. 6. It is evident that the directivity of the proposed method is comparable to that of differential arrays. It should be emphasized that the theoretical upper directivity limit, M^2 , is valid for arrays of omni-directional sensors. It is not applicable to the proposed method that is based on directional velocity sensors.

The proposed beamformer is a derivative of gradient and differential microphone arrays. In essence, both methods are based on the estimation of the gradients of the acoustic field variables from closely spaced sensors. Since the proposed method represents a viable alternative to omni-directional pressure sensor based differential arrays, it is worth comparing the directivity of the two methods. One of the most significant attributes of the proposed method is the reduction in the array aperture due to smaller sensor spacing. This reduction in the aperture can be quantified by comparison to the required aperture for an equivalent conventional array. Equivalence between the arrays is defined in terms of the DF. The results are depicted in Fig. 8 where the apertures are given in terms of the wavelength. The sensor spacing for the conventional and proposed arrays are $\lambda/2$ and $\lambda/10$, respectively. The proposed method attains a performance equivalent to a conventional array with 70%–85% shorter apertures. However, the difference in aperture lengths decreases as the number of sensors in the array increases. Finally, it should be noted that although the proposed method achieves equivalent performance with a

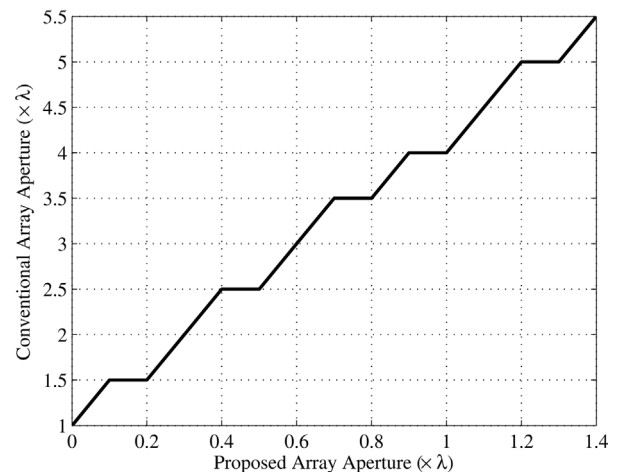


FIG. 8. A comparison between the required apertures for a conventional pressure array and an equivalent gradient vector sensor array (proposed method). Aperture lengths are given in terms of the wavelength (λ).

shorter aperture, just as with most AVS arrays, the resulting array will have higher data processing loads due to higher number of sensor channels.

E. Alternative configurations

The proposed beamformer relies on a linear array of closely spaced 2-D particle velocity sensors and a single pressure sensor. The velocity measurements in the direction of the array axis (x -axis) provide the cosine modes. The velocity measurements in the y -direction provide the sine modes. Extracting both cosine and sine modes enables the array response to be steered to any desired azimuthal direction. This ability to steer in the azimuth without distorting the array response is what separates the proposed method from existing literature on differential microphone arrays and subtractive endfire arrays. It is noted in Sec. II that a single pressure measurement, made at array center, is necessary to obtain the desired array response.

Alternatively, the beamformer can also be implemented for a linear array of one-dimensional (1-D) AVS. The AVS utilized in this configuration are capable of making collocated measurements of the pressure and the y -direction particle velocity. For the justification of this alternative configuration, first note from Eq. (1) that the x -direction spatial gradients of the pressure field are

$$\frac{\partial^n p}{\partial x^n} = P(jk)^n (\cos \psi)^n \exp(jk \cos \psi x). \quad (26)$$

Evaluated at the origin, the pressure gradients become

$$\frac{\partial^n p}{\partial x^n}(0) = P(jk)^n (\cos \psi)^n. \quad (27)$$

Note also that the pressure gradients given in Eq. (27) and the x -direction velocity gradients [given in the first line of Eq. (3)] are similar in the sense that both can be utilized to obtain the cosine modes of the acoustic field. The main difference between the n th order pressure and n th order x -direction particle velocity gradients is that the order of the former is one less than that of the latter. Thus, it is possible to apply the same beamforming procedure on a linear array of 1-D AVS. With an array of M 2-D velocity sensors, it is possible to extract $N = M - 1$ cosine modes. In contrast, only $N = M - 2$ cosine modes can be extracted from an array of M 1-D AVS. Since directivity increases with the number of modes extracted, a 1-D AVS array will have lower directivity compared to an array of equal numbered 2-D velocity sensors.

IV. CONCLUSIONS

A subtractive beamformer for short vector sensor arrays is presented in this paper. The presented method is based on the extraction of the directional modes of the acoustic field from finite difference based approximations of the particle velocity gradients. The resulting beamformer has some very desirable attributes such as super-directivity, ability to steer the main response axis, steering and frequency independent response, and front-back (port-starboard) discrimination.

The processing is similar to existing differential or gradient pressure sensor arrays, with the exception being that the gradients of particle velocity (and not pressure) are employed. 2-D particle velocity measurements in the plane of the array result in two sets of orthogonal modes, enabling array steering without distortion in the beam pattern or loss in directivity. Thus, the limitation of not being able to steer the main response axis away from the endfire direction present in differential arrays is overcome. The directivity of the proposed method is comparable to the maximum directivity that can be achieved with differential microphone arrays with similar aperture length.

Unlike conventional delay-and-sum pressure sensor and AVS arrays, very small inter-sensor spacing is required for the proposed method. As a consequence, a significant reduction in the array aperture is possible. Theoretical calculations and numerical simulations reveal that 70%–85% shorter apertures (relative to conventional arrays) with equal number of sensors are sufficient to achieve comparable directivity. Owing to this shorter aperture and other potential operational advantages, the proposed method is suitable for use in space constrained applications such as hearing aids and short towed arrays with autonomous underwater platforms.

The development presented in this paper is based on the assumption of a 2-D acoustic field. Although the extension to 3-D is not straightforward, it appears to be possible and is currently under investigation. The directivity of the proposed beamformer is expected to decrease in the presence of uncorrelated noise (in particular, at low frequencies). Thus, the effects of uncorrelated noise on beamformer performance and the white noise gain of the array should be analyzed. One of the primary applications of arrays is DOA estimation. Measurements from the vector sensors of the array are readily available and can be used to implement existing DOA methods. However, novel and improved DOA estimation techniques that exploit the gradients of the acoustic field are worth investigating. Finally, the practical realization of the proposed method is investigated through ongoing experiments conducted using an array of six in-air 2-D particle velocity sensors with an aperture of 25 cm.

ACKNOWLEDGMENTS

The author would like to thank to Dr. Hans-Elias de Bree from Microflown Technologies and Dr. Tuncay Akal from SUASIS Underwater Systems for providing the motivation for this work. The author would also like to express his sincere appreciation to the European Commission FP7 PEOPLE Marie Curie Actions Program for supporting this research (Grant No. PIRG-GA-2009-256585).

APPENDIX: CLOSED FORM EXPANSIONS OF THE VELOCITY GRADIENTS [DERIVATION OF EQS. (7) AND (8)]

Using Euler's formula, $\cos \psi$ can be expressed as

$$\cos \psi = \frac{\exp(j\psi) + \exp(-j\psi)}{2}, \quad (A1)$$

and $(\cos \psi)^{n+1}$ as

$$(\cos \psi)^{n+1} = \frac{1}{2^{n+1}} [\exp(j\psi) + \exp(-j\psi)]^{n+1}. \quad (\text{A2})$$

Using the binomial theorem (Abramowitz and Stegun, 1972), Eq. (A2) can be expressed as

$$(\cos \psi)^{n+1} = \frac{1}{2^{n+1}} \sum_{l=0}^{n+1} \binom{n+1}{l} [\exp(j\psi)]^{n+1-l} [\exp(-j\psi)]^l = \frac{1}{2^{n+1}} \sum_{l=0}^{n+1} \binom{n+1}{l} \exp[j(n-2l+1)\psi]. \quad (\text{A3})$$

Note that if $n+1$ is even, the summation in Eq. (A3) can be divided into three terms,

$$(\cos \psi)^{n+1} = \frac{1}{2^{n+1}} \left[\sum_{l=0}^{(n-1)/2} \binom{n+1}{l} \exp[j(n-2l+1)\psi] + \binom{n+1}{(n+1)/2} + \sum_{l=(n+3)/2}^{n+1} \binom{n+1}{l} \exp[j(n-2l+1)\psi] \right]. \quad (\text{A4})$$

A careful examination of Eq. (A4) will reveal that the first and last terms in the summation can be merged into a single summation of cosine functions,

$$\sum_{l=0}^{(n-1)/2} \binom{n+1}{l} \exp[j(n-2l+1)\psi] + \sum_{l=(n+3)/2}^{n+1} \binom{n+1}{l} \exp[j(n-2l+1)\psi] = \frac{2}{2^{n+1}} \sum_{l=0}^{(n-1)/2} \binom{n+1}{l} \cos[(n-2l+1)\psi], \quad (\text{A5})$$

resulting in

$$(\cos \psi)^{n+1} = \frac{2}{2^{n+1}} \sum_{l=0}^{(n-1)/2} \binom{n+1}{l} \cos[(n-2l+1)\psi] + \frac{1}{2^{n+1}} \binom{n+1}{(n+1)/2}. \quad (\text{A6})$$

If $n+1$ is odd, the summation can be separated into two as

$$(\cos \psi)^{n+1} = \frac{1}{2^{n+1}} \left[\sum_{l=0}^{n/2} \binom{n+1}{l} \exp[j(n-2l+1)\psi] + \sum_{l=(n+2)/2}^{n+1} \binom{n+1}{l} \exp[j(n-2l+1)\psi] \right]. \quad (\text{A7})$$

The two summations of Eq. (A7) can be merged into a single summation of cosines resulting in

$$(\cos \psi)^{n+1} = \frac{2}{2^{n+1}} \sum_{l=0}^{n/2} \binom{n+1}{l} \cos[(n-2l+1)\psi]. \quad (\text{A8})$$

Equations (A6) and (A8) are the equations given in Eq. (7).

One can expand the term $\sin \psi (\cos \psi)^n$ as

$$\sin \psi (\cos \psi)^n = \frac{1}{2j} [\exp(j\psi) - \exp(-j\psi)] \frac{1}{2^n} [\exp(j\psi) + \exp(-j\psi)]^n, \quad (\text{A9})$$

and invoking the binomial theorem on the latter term, Eq. (A9) becomes

$$\sin \psi (\cos \psi)^n = \frac{1}{2j} \frac{1}{2^n} [\exp(j\psi) - \exp(-j\psi)] \sum_{l=0}^n \binom{n}{l} [\exp(j\psi)]^{n-1} [\exp(-j\psi)]^l, \quad (\text{A10})$$

or equivalently,

$$\begin{aligned} \sin \psi (\cos \psi)^n &= \frac{1}{2^n} \frac{1}{2j} [\exp(j\psi) - \exp(-j\psi)] \sum_{l=0}^n \binom{n}{l} \exp[j(n-2l)\psi] \\ &= \frac{1}{2^n} \frac{1}{2j} \sum_{l=0}^n \binom{n}{l} \{ \exp[j(n-2l+1)\psi] - \exp[-j(n-2l-1)\psi] \}. \end{aligned} \quad (\text{A11})$$

Due to the symmetry of the binomial terms, the summation of two exponential terms in Eq. (A11) can be simplified to a summation of sine terms. If n is odd, the summation simplifies to

$$\sin \psi (\cos \psi)^n = \frac{1}{2^n} \sum_{l=0}^{(n-1)/2} \left[\frac{n!(n-2l+1)}{l!(n-l+1)!} \right] \times \sin[(n-2l+1)\psi]. \quad (\text{A12})$$

If n is even, the summation becomes

$$\sin \psi (\cos \psi)^n = \frac{1}{2^n} \sum_{l=0}^{n/2} \left[\frac{n!(n-2l+1)}{l!(n-l+1)!} \right] \times \sin[(n-2l+1)\psi]. \quad (\text{A13})$$

Equations (A12) and (A13) are the equations given in Eq. (8). Note that the coefficients of the sine terms are computed from

$$\binom{n}{l} - \binom{n}{l-1} = \left[\frac{n!(n-2l+1)}{l!(n-l+1)!} \right]. \quad (\text{A14})$$

- Abhayapala, T. D., and Gupta, A. (2010). "Higher order differential-integral microphone arrays," *J. Acoust. Soc. Am.* **127**(5), 227–233.
- Abramowitz, M., and Stegun, I. A. (1972). *Handbook of Mathematical Functions with Formulas, Graphs, and Mathematical Tables*, 9th ed. (Dover, New York), Chap. 3, pp. 9–64.
- Chen, H. W., and Zhao, J. W. (2004). "Wideband MVDR beamforming for acoustic vector sensor linear array," *IEE Proc. Radar Sonar Navig.* **151**(3), 158–162.
- Chung, K., Zeng, F. G., and Acker, K. N. (2006). "Effects of directional microphone and adaptive multichannel noise reduction algorithm on cochlear implant performance," *J. Acoust. Soc. Am.* **120**(4), 2216–2227.
- Clark, J. A. (2008). "Higher-order angular response beamformer for vector sensor arrays," *J. Sound Vib.* **318**, 417–422.
- Cox, H., and Lai, H. (2007). "Performance of line arrays of vector and higher order sensors," in *Proc. 41st Asilomar Conf. Signals, Syst. Comput.*, pp. 1231–1236.
- Cox, H., and Lai, H. (2009). "Simultaneous grating lobe and backlobe rejection with a line array of vector sensors," in *Proc. 43rd Asilomar Conf. Signals, Syst. Comput.*, pp. 1320–1323.
- Cray, B. A., Evora, V. M., and Nuttall, A. H. (2003). "Highly directional acoustic receivers," *J. Acoust. Soc. Am.* **113**(3), 1526–1532.
- Cray, B. A., and Nuttall, A. H. (2001). "Directivity factors for linear arrays of velocity sensors," *J. Acoust. Soc. Am.* **110**(1), 324–331.
- De Sena, E., Hacıhabiboglu, H., and Cvetkovic, Z. (2012). "On the design and implementation of higher order differential microphones," *IEEE Trans. Audio Speech Language Process.* **20**(1), 162–174.
- D'Spain, G. L., Luby, J. C., Wilson, G. R., and Gramann, R. A. (2006). "Vector sensors and vector sensor line arrays: Comments on optimal array gain and detection," *J. Acoust. Soc. Am.* **120**(1), 171–185.

- Elko, G. W. (1996). "Microphone array systems for hands free tele-communications," *Speech Commun.* **20**, 229–240.
- Elko, G. W. (2004). "Differential microphone arrays," in *Audio Signal Processing for Next-Generation Multimedia Communication Systems*, edited by Y. Huang and J. Benesty (Kluwer, New York), pp. 11–65.
- Franklin, J. B. (1997). "Superdirective receiving arrays for underwater acoustic application," DREA Contractor Report 97/444, P.O. Box 1012, Dartmouth, Nova Scotia, Canada B2Y 3Z7, pp. 1–44.
- Hawkes, M., and Nehorai, A. (1998). "Acoustic vector sensor beamforming and capon direction estimation," *IEEE Trans. Signal Process.* **46**(9), 2291–2304.
- Jacobsen, F., and de Bree, H. E. (2009). "The microflown particle velocity sensor," in *Handbook of Signal Processing in Acoustics*, edited by D. Havelock, S. Kuwano, and M. Vorlander (Springer, New York), pp. 1283–1291.
- Kasilingam, D., Schmidlin, D., and Pacheco, P. (2009). "Super-resolution processing technique for vector sensors," in *Proc. IEEE Radar Conf.*, pp. 1–4.
- Kates, J. M. (1993). "Superdirective arrays for hearing aids," *J. Acoust. Soc. Am.* **94**(4), 1930–1933.
- Kolundzija, M., Faller, C., and Vetterli, M. (2011). "Spatiotemporal gradient analysis of differential microphone arrays," *J. Audio Eng. Soc.* **59**(1/2), 20–28.
- Krim, H., and Viberg, M. (1996). "Two decades of array signal processing research: The parametric approach," *IEEE Signal Process. Mag.* **13**(4), 67–94.
- Lai, H., and Bell, K. (2007). "Cramer–Rao lower bound for DOA estimation using vector and higher-order sensor arrays," in *Proc. 41st Asilomar Conf. Signals, Syst. Comput.*, pp. 1262–1266.
- Nehorai, A., and Paldi, E. (1994). "Acoustic vector-sensor array processing," *IEEE Trans. Signal Process.* **42**(9), 2481–2491.
- Olson, H. (1946). "Gradient microphones," *J. Acoust. Soc. Am.* **17**(3), 192–198.
- Parsons, A. T. (1987). "Maximum directivity proof for three-dimensional arrays," *J. Acoust. Soc. Am.* **82**(1), 179–182.
- Schmidlin, D. J. (2007). "Directionality of generalized acoustic sensors of arbitrary order," *J. Acoust. Soc. Am.* **121**(6), 3569–3578.
- Shiggs, J. C., and Deng, K. (2003). "A miniature vector sensor for line array applications," *Proc. Oceans* **5**, 2367–2370.
- Smith, K. B., and Van Leijen, A. V. (2007). "Steering vector sensor array elements with linear cardioids and nonlinear hippoids," *J. Acoust. Soc. Am.* **122**(1), 370–377.
- Song, Y., and Wong, K. T. (2012). "Closed-form direction finding using collocated but orthogonally oriented higher order acoustic sensors," *IEEE Sensors J.* **12**(8), 2604–2608.
- Teutsch, H. (2007). *Modal Array Signal Processing: Principles and Applications of Acoustic Wavefield Decomposition* (Springer, Berlin), Chap. 4, pp. 95–148.
- Thompson, S. C. (2003). "Tutorial on microphone technologies for directional hearing aids," *Hear. J.* **56**(11), 14–21.
- Van Veen, B. D., and Buckley, K. M. (1988). "Beamforming: A versatile approach to spatial filtering," *IEEE ASSP Mag.* **5**(2), 4–24.
- Weston, D. E. (1986). "Jacobi sensor arrangement for maximum array directivity," *J. Acoust. Soc. Am.* **80**(4), 1170–1181.
- Ziomek, L. J. (1995). *Fundamentals of Acoustic Field Theory and Space-Time Signal Processing* (CRC Press, Boca Raton, FL), Chap. 2, pp. 47–150.